Fragmentation of Vitamin B_{12} in Aerosol Matrix-Assisted Laser Desorption Ionization

Lin He, Gang Wei, and Kermit K. Murray
Department of Chemistry, Emory University, Atlanta, Georgia, USA

Aerosol matrix-assisted laser desorption ionization (MALDI) with a reflectron time-of-flight mass spectrometer was used to study fragmentation of vitamin B_{12}. Six MALDI matrices were used: 2,5-di-hydroxy benzoic acid (gentisic acid), 4-nitroaniline, 3,5-dimethoxy-4-hydroxy cinnamic acid (sinapic acid), 3,4-di-hydroxy cinnamic acid (caffeic acid), *trans*-4-hydroxy-3-methoxy cinnamic acid (ferulic acid), and α-cyano-4-hydroxy cinnamic acid (4-HCCA). Mass spectra were obtained with a 355-nm pulsed Nd:YAG laser at irradiances between 0.1 and 5 GW/cm^2 (between 3- and 150-mJ pulse energy). Loss of CN was a major product of prompt ion source fragmentation and the ratio of fragmented to intact analyte was found to be strongly dependent on matrix and weakly dependent on laser irradiance. Additionally, free cobalt ions and cobalt ions bound to small methanol clusters were observed in the mass spectra. The cobalt removal from the corrin ring of vitamin B_{12} results from direct photon absorption by vitamin B_{12}, but is enhanced by the presence of matrix.
 (J Am Soc Mass Spectrom 1997, 8, 140–147)

Matrix-assisted laser desorption ionization (MALDI) is a useful method for molecular weight determination of peptides and proteins in part because protonated analyte molecules are produced without extensive fragmentation [1, 2]. However, there are cases where fragmentation does occur and the resulting data can be useful for obtaining analyte structural information. MALDI postsource decay (PSD) is fragmentation that results either from unimolecular or from background gas collision-induced dissociation [3]. The delayed fragmentation associated with PSD can be used for sequencing peptides with a reflectron time-of-flight (TOF) mass spectrometer [4]. For less stable analytes, fragmentation occurs in the ion source on a relatively fast time scale. For example, MALDI of gangliosides results in prompt fragmentation that provides useful structural information [5]. It was recently discovered that when extraction of ions from the source is delayed by several hundred nanoseconds, ion source fragmentation of peptides and proteins can be observed [6].

There are some cases where minimizing analyte fragmentation in MALDI is crucial in obtaining mass spectra. For example, there is a growing body of evidence that suggests that prompt fragmentation of oligonucleotides and DNA in the ion source on a 0.1–1-μs time scale is the limiting factor for mass resolution, detection limit, and upper mass limit [7–10]. Experiments demonstrating desorption of neutral radio-labeled DNA over 1000 nucleotides in length give evidence that dissociation occurs during the ionization, rather than the desorption, step [11, 12]. In some DNA ionization experiments, a higher than typical acceleration voltage was used to minimize the time the ions spend in the acceleration region, and thus minimize the effect of fragmentation [13, 14]. A better understanding of MALDI fragmentation mechanisms can potentially lead to improved analysis methods for DNA and other thermally labile analytes.

Vitamin B_{12} is a good analyte molecule for investigating MALDI fragmentation: it is readily fragmented and has been studied by a variety of mass spectrometric techniques. For example, vitamin B_{12} has been observed by ^{252}Cf plasma desorption (PDMS) [15] and field desorption (FD) mass spectrometry [16]. The fast-atom bombardment (FAB) mass spectra of several cobalamines including vitamin B_{12} (cyano cobalamine) show an intense peak at m/z 1329 corresponding to the loss of the axially attached ligand, which is CN in the case of vitamin B_{12} [17]. Fragmentation also occurs on the side chain bound to the cobalt atom. Vitamin B_{12} has been used in a comparison of FAB and PDMS [18], and Fourier transform mass spectrometry was used to investigate fragmentation of vitamin B_{12} by MALDI and by gas phase photodissociation [19]. Prompt matrix specific fragmentation of vitamin B_{12} was observed with a linear TOF mass spectrometer and the matrices α-cyano-4-hydroxy cinnamic acid (4-HCCA) and 4-hydroxy-3-iodo-5-nitrobenzoic acid [20].

Aerosol MALDI represents a new and unique perspective from which to study the fundamentals of the MALDI process. In the aerosol MALDI method, a solution of matrix and analyte is sprayed directly into

Address reprint requests to Kermit K. Murray, Department of Chemistry, Emory University, Atlanta, GA 30322.

1044-0305/97/$17.00
PII S1044-0305(96)00230-9

Received June 24, 1996
Revised September 30, 1996
Accepted September 30, 1996

a TOF mass spectrometer and ionized by pulsed laser radiation [21, 22]. Because aerosol particles are directly ionized, substrate effects are not present as they can be in conventional MALDI that uses a solids probe. The sample is continuously renewed; therefore, the effects of sample depletion and spot-to-spot signal variation are not present. Additionally, mass spectra can be obtained over a wide range of laser irradiances, typically more than 2 orders of magnitude, facilitating laser irradiance dependence studies [22]. The fundamental process that leads to ion formation in aerosol MALDI is similar to that of solids probe MALDI: analyte ion formation does not occur without a matrix and the most intense high mass signal for most analytes is the protonated molecule [21–23]. Some of the differences between aerosol and solids probe MALDI have been ascribed to differences in matrix and analyte crystal formation processes [23, 24].

In this article, an aerosol MALDI investigation of the matrix-specific fragmentation of vitamin B_{12} is described. Six MALDI matrices were used: 2,5-di-hydroxy benzoic acid (gentisic acid), 4-nitroaniline, and four cinnamic acid derivatives—3,5-dimethoxy-4-hydroxy cinnamic acid (sinapic acid), 3,4-di-hydroxy cinnamic acid (caffeic acid), *trans*-4-hydroxy-3-methoxy cinnamic acid (ferulic acid), and α-cyano-4-hydroxy cinnamic acid (4-HCCA) [25–27]. Mass spectra were obtained over a range of 355-nm laser irradiances from the threshold for ion observation at 0.1 up to 5 GW/cm^2.

Experimental

The aerosol MALDI reflectron TOF mass spectrometer was described in detail previously [22]. A methanol solution of matrix and analyte was sprayed into vacuum by using a pneumatic nebulizer with nitrogen carrier gas. Typical liquid flow rates were 0.5 mL/min. Solvent was removed as the particles passed through a heated drying tube and ions were formed with 10-Hz pulsed 355-nm radiation from a frequency tripled Nd:YAG laser. The Gaussian laser beam was focused to a 5-mm × 0.1-mm spot by using a cylindrical lens; the long axis was parallel to the aerosol beam. This spot size represents the contour of 50% of maximum irradiance in the Gaussian beam [22]. At a typical pulse energy of 100 mJ, the laser fluence was 20 J/cm^2 and the irradiance of the 6-ns pulse was 3 GW/cm^2 obtained using the 5-mm × 0.1-mm spot size. An acceleration voltage of 10 kV was used to extract the ions formed by laser irradiation. Ions were formed at the midpoint of the single stage acceleration region; thus the ion energies were 5 kV. A two stage reflectron was used for mass separation and the detector was a 40-mm dual microchannel plate particle multiplier. The detector signal output was sent to a 500-MHz digital oscilloscope that was triggered by the laser Q-switch signal. Averaged mass spectra were transferred from the oscilloscope to a microcomputer for analysis. The mass spectra shown in this article resulted from an average of 100 to 1000 single mass spectra with a 1-ns data point spacing. Peak areas were determined by numerical integration and peak widths were determined by a nonlinear least squares fit to a Gaussian functional form. Mass spectra were software boxcar averaged to reduce the number of data points for plotting [22].

Sample solutions were made from matrix and analyte dissolved in methanol (99.8%, EM Science, Gibbstown, NJ) with 5% trifluoroacetic acid (Baker, Phillipsburg, NJ) by volume. For all of the mass spectra reported, the solutions contained 1 mg/mL of analyte and 4 mg/mL of matrix. The matrix compounds 2,5-di-hydroxy benzoic acid (gentisic acid, Sigma Chemical Co., St. Louis, MO), 4-nitroaniline (99%, Fluka, Ronkonkoma, NY), 3,5-dimethoxy-4-hydroxy cinnamic acid (sinapic acid, 98%, Fluka), 3,4-dihydroxy cinnamic acid (caffeic acid, 97%, Aldrich Chemical Co., Milwaukee, WI), *trans*-4-hydroxy-3-methoxy cinnamic acid (ferulic acid, 99%, Aldrich), and α-cyano-4-hydroxy cinnamic acid (Sigma), and the analyte vitamin B_{12} (99%, V-2876; Sigma) were used without further purification.

Results

The goal of this study was to investigate the effects of different matrix molecules and different laser irradiances on the fragmentation of vitamin B_{12} in aerosol MALDI. Vitamin B_{12} was chosen as the analyte because its fragmentation is sensitive to the specific ionization conditions, making it a suitable "molecular thermometer" [15–20]. The six matrices used in this experiment are standard MALDI matrices: 2,5-dihydroxy benzoic acid (gentisic acid) [25], 4-nitroaniline [26], 3,5-dimethoxy-4-hydroxy cinnamic acid (sinapic acid) [25], 3,4-dihydroxy cinnamic acid (caffeic acid) [25], *trans*-4-hydroxy-3-methoxy cinnamic acid (ferulic acid) [25], and α-cyano-4-hydroxy cinnamic acid (4-HCCA) [27]. The laser irradiance was varied from the threshold for aerosol MALDI ion detection of approximately 100 MW/cm^2 up to 5 GW/cm^2.

An aerosol MALDI reflectron TOF spectrum of vitamin B_{12} with α-cyano-4-hydroxy cinnamic acid as the matrix is shown in Figure 1. The spectrum is an average of 1000 laser shots at an irradiance of 0.2 GW/cm^2. A 20-point boxcar average was performed on the data for plotting. The relatively intense ion signal between 10- and 50-μs results primarily from protonated and singly charged cobalt containing methanol clusters of the form $H^+(CH_3OH)_n$ and $Co^+(CH_3OH)_n$. The peak at 88.6 μs corresponds to the singly protonated vitamin B_{12} and is labeled $[M + H]^+$. The peak at 87.7 μs is labeled $[M - CN + H]^+$ and corresponds to the protonated fragment of a vitamin B_{12} molecule that results from the loss of a CN ligand. The $[M - CN + H]^+$ peak results from ion source fragmentation and has been observed previously in solids probe MALDI [20]. The $[M + H]^+$ peak is observed at 1356.1 u and

the $[M - CN + H]^+$ peak is observed at 1330.1 u when the spectra are calibrated by using the methanol clusters as an internal standard. The mass resolution for the $[M - CN + H]^+$ and $[M + H]^+$ peaks in Figure 1 is approximately $m/\Delta m = 380$ full width at half maximum (FWHM) and the mass measurement accuracy is 0.05%. Analyte ion formation proceeds by a MALDI process: neither the $[M + H]^+$ nor the $[M - CN + H]^+$ peaks appear in spectra from aerosol solutions that do not contain matrix. The peak at 92 μs is tentatively identified as an adduct of trifluoroacetic acid with vitamin B_{12}. The mass-to-charge ratio of the peak is 1443 and it appears in spectra of vitamin B_{12} with several matrix molecules. When the aerosol solution is acidified by acetic acid rather than trifluoroacetic acid, the peak at 92 μs disappears and no new peaks appear. The broad peak at 67 μs results from post-source decay (PSD) of the vitamin B_{12} due to metastable or collision-induced fragmentation in the flight tube. No resolved PSD peaks are observed: all of the peaks in the spectral region between the unresolved PSD peak and the $[M + H]^+$ and the $[M - CN + H]^+$ peaks can be assigned to vitamin B_{12} fragments observed either in solids probe MALDI or FAB [17–20] or to demetalated vitamin B_{12}, $[M - Co + H]^+$. Additionally, resolved PSD peaks can be easily identified by changing the reflectron voltage while maintaining a constant acceleration voltage [22]. No such peaks were observed.

An expanded region of a vitamin B_{12} mass spectrum in the low mass region is shown in Figure 2. This region of the mass spectrum is dominated by protonated methanol clusters $H^+(CH_3OH)_n$ and methanol clusters containing a cobalt ion $Co^+(CH_3OH)_n$. Isotopic resolution is observed in this region of the mass spectrum; thus identification of the cluster ion peaks is straightforward. The protonated methanol clusters have been observed previously [23] and are a common feature in aerosol MALDI mass spectra and often are used for mass calibration [22]. Cobalt-containing clusters in vitamin B_{12} mass spectra have not been reported; however, methanol clusters containing Fe^+ were observed in the aerosol MALDI mass spectrum of the heme protein myoglobin [28]. In the region of the mass spectrum between 150 and 350 u, peaks corresponding to clusters of between three and nine methanol molecules, a single water molecule, and either a cobalt ion or proton are seen [$H^+ \cdot H_2O(CH_3OH)_n$ and $Co^+H_2O(CH_3OH)_n$]. Both protonated and cobalt ion-containing methanol clusters are formed from solutions containing vitamin B_{12} but no matrix, although at approximately 10 times lower signal intensity. Thus at least some of the $Co^+(CH_3OH)_n$ clusters are formed as a result of direct photon absorption by vitamin B_{12}, although the process is enhanced by the presence of matrix. Protonated methanol clusters are formed from solutions containing only methanol and TFA, although the signal is weaker than that from solutions containing vitamin B_{12}. These results suggest that the methanol clusters are formed by direct laser desorption of the aerosol particles, but formed more efficiently if there is a photon absorber in the solution.

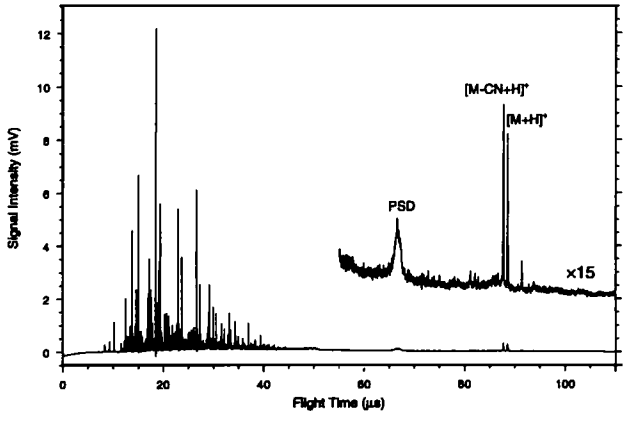

Figure 1. Aerosol MALDI reflectron TOF spectrum of vitamin B_{12} with α-cyano-4-hydroxy cinnamic acid as the matrix.

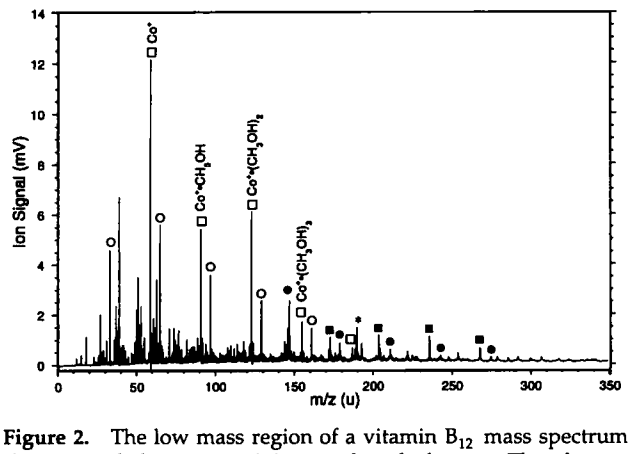

Figure 2. The low mass region of a vitamin B_{12} mass spectrum showing cobalt ion-containing methanol clusters. The clusters $Co^+ \cdot (CH_3OH)_n$ are indicated by open boxes, the clusters $H^+ \cdot (CH_3OH)_n$ are indicated by open circles, and the clusters $H^+ \cdot H_2O \cdot (CH_3OH)_n$ and $Co^+ \cdot H_2O \cdot (CH_3OH)_n$ are indicated by solid circles and solid boxes, respectively. The peak labeled with the asterisk corresponds to the protonated α-cyano-4-hydroxy cinnamic acid matrix.

The intermediate mass region of a vitamin B_{12} mass spectrum with 4-HCCA matrix is shown in Figure 3. The laser irradiance was 1.2 GW/cm^2 and a 10-point boxcar average was performed for plotting. Prominent fragment peaks observed at m/z 1298, 1271, 1168, 1139, and 944 correspond to axial and corrin ring side chain fragmentation [17–20]. The mass measurement accuracy for these lower intensity peaks is approximately 0.1%. With the exception of the peak at m/z 1298, which we assign as the loss of cobalt to form $[M - Co + H]^+$, these peaks are observed in FAB mass spectrometry of vitamin B_{12} [17]. The m/z 972 peak has been observed in solids probe MALDI of vitamin B_{12} [20]. Like the CN loss fragment, these intermediate mass fragments are formed in the ion source on a

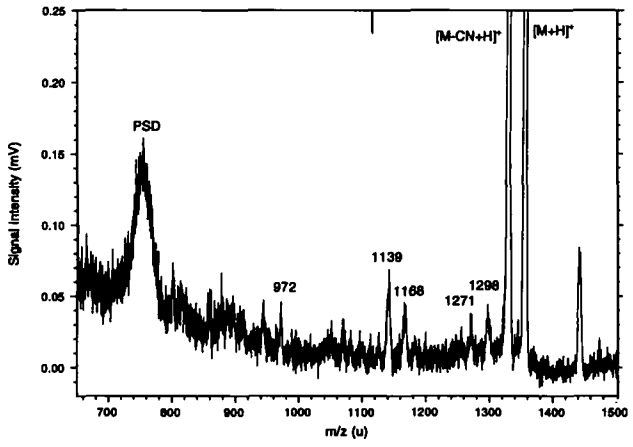

Figure 3. Aerosol MALDI mass spectrum of vitamin B_{12} showing prompt fragmentation peaks.

prompt time scale. An upper bound to the time of ion formation is the width of the fragment peak in the TOF spectrum [29]. The fragment peaks in the TOF spectra are approximately 100 ns wide FWHM; thus ion formation cannot be occurring for longer than approximately 100 ns. The matrix 4-HCCA gives the best signal-to-noise ratio for the prompt fragmentation peaks. At high laser irradiances, these intermediate mass prompt fragments ions are present in all mass spectra, regardless of matrix.

Figure 4 shows mass spectra of vitamin B_{12} obtained with different matrix molecules: 4-nitroaniline, 4-HCCA, sinapic acid, ferulic acid, caffeic acid, and gentisic acid. The spectra were obtained at a laser irradiance of 0.1 GW/cm^2 and a 20-point boxcar average was performed on the data for plotting. The spectra were normalized to the height of $[M - CN + H]^+$ peaks and the mass resolution based on this peak is approximately $m/\Delta m = 400$ for all of the mass spectra. The spectra show general features of vitamin B_{12} spectra in Figures 1–3, but there are several features unique to the individual mass spectra. The $[M - CN + H]^+$ peak area shows some variation from matrix to matrix: 4-HCCA generates the largest $[M - CN + H]^+$ peak area, which is typically a factor of 2 larger than that of gentisic acid, caffeic acid, and 4-nitroaniline, and three times larger than that of sinapic and ferulic acids. The most striking difference among the spectra is the relative intensities of the $[M + H]^+$ and $[M - CN + H]^+$ peaks. The matrices 4-nitroaniline and 4-HCCA give $[M + H]^+$ peaks nearly as intense as the $[M - CN + H]^+$ peak. Sinapic, ferulic, and caffeic acids produce relatively weaker $[M + H]^+$ peaks, approximately one third as intense as the $[M - CN + H]^+$ peak. The matrix gentisic acid produces no $[M + H]^+$ peak that can be distinguished from baseline noise. The different matrices also give different amounts of postsource decay. Taking the ratio of the unresolved PSD peak to the $[M - CN + H]^+$ peak as an indication, 4-nitroaniline and 4-HCCA generate the most PSD, and sinapic acid the least.

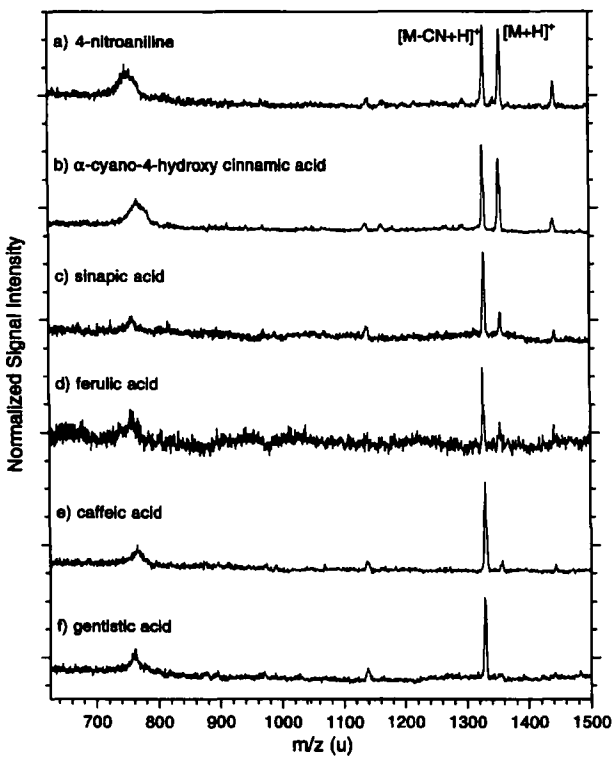

Figure 4. Aerosol MALDI reflectron TOF mass spectra of vitamin B_{12} by using the matrices (a) 4-nitroaniline, (b) α-cyano-4-hydroxy cinnamic acid, (c) sinapic acid, (d) ferulic acid, (e) caffeic acid, and (f) gentisic acid.

Mass spectra of vitamin B_{12} with sinapic acid matrix at different laser irradiances are shown in Figure 5. Each mass spectrum is an average of 1000 laser shots and the spectra were normalized to the height of $[M - CN + H]^+$ peaks. Two results are apparent as the laser irradiance is increased: a decrease and finally disappearance of the $[M + H]^+$ signal and a broadening of the $[M - CN + H]^+$ peak. These trends are observed for all matrices (although note that gentisic acid does not produce a detectable $[M + H]^+$ ion signal). At the lowest laser irradiance, the sinapic acid spectra in Figure 5 show a relatively small $[M + H]^+$ peak. Above 2-GW/cm^2 laser irradiance the $[M + H]^+$ peak is no longer distinguishable from baseline. In Figure 5, as laser irradiance is increased from 0.1 to 5 GW/cm^2, the width of $[M - CN + H]^+$ peak increases from 110 to 180 ns (peak widths were determined by a least squares fit to a Gaussian functional form). Correspondingly, the mass resolution decreases from 430 to 240. Peak broadening at high laser irradiances has been observed previously in aerosol MALDI with a reflectron [22]. Data similar to that depicted in Figure 5 were obtained over a range of laser irradiance between 0.1 and 5 GW/cm^2 for the six matrices used. The general result for the six matrices used in this experiment is that the $[M - CN + H]^+$ (and $[M + H]^+$, when present) peak width increases by a factor of between 2 and 3 when the laser irradiance is increased from 0.1 to 5 GW/cm^2. For all of the matrices used, the

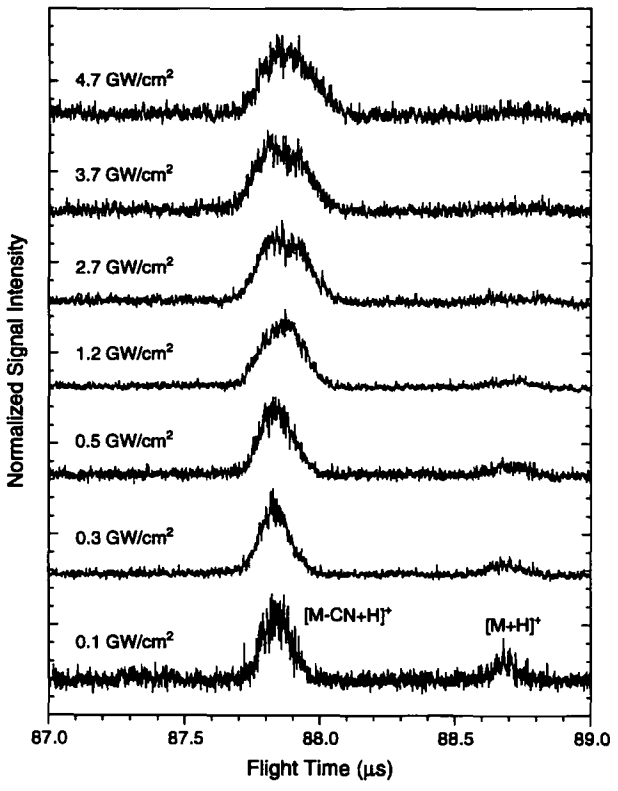

Figure 5. Aerosol MALDI reflectron TOF mass spectra of vitamin B_{12} with a sinapic acid matrix at different laser irradiances.

$[M + H]^+$ and $[M - CN + H]^+$ peak widths scale with approximately the one-fourth power of the laser irradiance.

The laser irradiance data were also used to obtain the ratio of the $[M - CN + H]^+$ to $[M + H]^+$ peak areas. The peak areas were determined by numerical integration of uncalibrated spectra. Figure 6 shows a logarithmic plot of the $[M - CN + H]^+$ to $[M + H]^+$ peak area ratio as a function of laser irradiance. Three matrices, 4-nitroaniline, caffeic acid, and sinapic acid, are shown for clarity. The lines through the data result from a least squares fit to the power law function $R = AE^n$, where R is the peak area ratio, E is the laser irradiance, n is the slope of the log-log plot, and A is a scaling factor. In this simple function, the magnitude of n gives an indication of how rapidly R changes with laser irradiance. For example, $n = 1$ indicates a linear irradiance dependence. For all of the matrices, the laser irradiance dependence is relatively weak, from $n = 0$ to a maximum of $n = 0.4$. The n values are the largest for the three matrices that give the most fragmentation: 0.41 for ferulic acid, 0.28 for sinapic acid, and 0.22 for caffeic acid. For the two matrices showing less CN loss fragmentation, R is relatively constant; thus n is small: $n = 0.15$ for 4-nitroaniline and $n = 0.06$ for 4-HCCA. The gentisic acid matrix did not give a measurable $[M + H]^+$ peak signal at any laser irradiance.

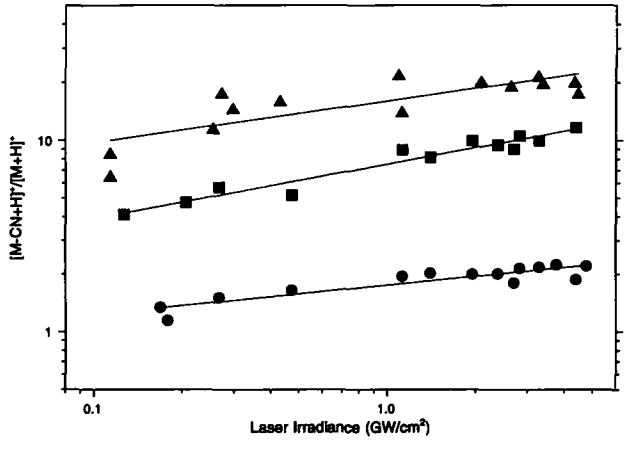

Figure 6. Log-log plot of the ratio of the $[M - CN + H]^+$ to $[M + H]^+$ peak area as a function of laser irradiance. The solid circle corresponds to 4-nitroaniline, the solid box corresponds to sinapic acid, and the solid triangle corresponds to caffeic acid.

Discussion

Several general statements may be made regarding the results. First, the vitamin B_{12} $[M - CN + H]^+$ and $[M + H]^+$ peak widths increase with increasing laser irradiance at a rate that is independent of the matrix used. Second, vitamin B_{12} loses cobalt from the corrin ring both by direct UV photon absorption and also by a matrix-assisted mechanism. Third, vitamin B_{12} shows different propensities for loss of the CN axial ligand, depending on the matrix used for ionization. The propensity for CN loss increases by approximately a factor of 2 with an order of magnitude increase in laser irradiance. Possible ionization mechanisms that are consistent with these results are discussed below.

Peak broadening at higher laser irradiance has been observed previously in the ionization of peptides by aerosol MALDI [22] (and also in solids probe MALDI [29], although over a smaller range of laser irradiances). It was postulated that higher laser irradiance used in aerosol MALDI could lead to increased spatial or temporal distribution of ions or to an increase in material ejected from the aerosol particles. All of these phenomena can lead to peak broadening. The peak width data from this study are similar to those of the previous aerosol MALDI study; however, a few statements can be made to add to the previous findings. First, the vitamin B_{12} peak width data are similar for all matrices tested, suggesting that whatever the mechanism for the peak broadening, it is not strongly matrix dependent. Second, by using reasonable values for the experimental parameters, ion spatial spread alone is insufficient to account for all of the peak broadening. Work is currently underway to further investigate the limiting factors for aerosol MALDI mass resolution.

The cobalt ions and Co^+ methanol clusters are formed both by direct photon absorption by vitamin B_{12} as well as in a process that is enhanced by the presence of matrix. The presence of Co^+ in mass spec-

tra of vitamin B_{12} by MALDI [19, 20], FAB [17, 18], or field desorption [16] has not been reported previously, although the ion $[M - Co]^+$ was observed in the field desorption mass spectrum. In a previous study, it was noted that Fe^+ and $Fe^+(CH_3OH)_n$ clusters were observed in the aerosol MALDI mass spectrum of the heme protein myoglobin [28]. It is difficult to speculate on the mechanism of Co^+ removal from the vitamin B_{12}, although it is possible that the process occurs in solution within the aerosol particle or in methanol clusters produced following irradiation of the particle. The presence of methanol solvent may serve to stabilize a cobalt ion removed from the corrin ring. It is likely that removal of the cobalt occurs in conjunction with photodestruction of the corrin ring, although a weak signal corresponding to demetalated vitamin B_{12} is observed in the aerosol MALDI mass spectra. Demetalation of the intact corrin ring in solution is achieved only under extremely harsh conditions, for example, by using concentrated HCl with excess 1,3-propanedithiol [30].

The most striking difference among the vitamin B_{12} mass spectra obtained with different matrices is the $[M - CN + H]^+$ to $[M + H]^+$ peak intensity ratio. The CN loss fragmentation is strongly dependent on matrix and weakly dependent on laser irradiance. It is somewhat surprising that extensive fragmentation cannot be induced, even at laser irradiances several orders of magnitude higher than the threshold for solids probe MALDI ion formation [1]. It may be, as has been proposed previously [23], that the analyte is cooled by solvent boil off from the aerosol particles and small clusters following irradiation. It is clear from this result that the matrix has a larger influence on the extent of fragmentation than does the laser irradiance.

The ratio of the $[M - CN + H]^+$ to $[M + H]^+$ peak areas gives an indication of the internal energy of the analyte in the few hundred nanoseconds following laser irradiation. Additionally, it is possible that different rates of metastable decay of the $[M - CN + H]^+$ to $[M + H]^+$ ions in the reflectron may influence the relative peak intensities. In both cases, a larger relative signal for the CN loss fragment is indicative of an analyte molecule with a relatively high internal energy. Based on the $[M - CN + H]^+$ to $[M + H]^+$ peak area ratio, the aerosol MALDI results indicate that 4-nitroaniline and 4-HCCA are "cold analyte" matrices and sinapic, ferulic, caffeic, and gentisic acids are "hot analyte" matrices. These results are not consistent with reported results for analyte activation in solids probe MALDI. For example, 4-HCCA has been shown to induce extensive PSD in MALDI of proteins [31] and was found to produce extensive prompt fragmentation of vitamin B_{12} in solids probe MALDI [20]. Thus 4-HCCA is typically regarded as a "hot analyte" matrix, which is inconsistent with the aerosol MALDI results. However, sinapic acid has been found to produce two to four times the drift region unimolecular decay as gentisic acid [3] and thus might be considered a "hot analyte" matrix, consistent with the results for sinapic but not gentisic acid. The Stokes shift of the UV transition at the wavelength used for MALDI has been suggested as one indication of the energy gained by the matrix molecule after photon absorption and thus might be related to its analyte activation ability [32]. A larger Stokes shift can be taken as indicative of a hotter matrix molecule. Based on the Stokes shift criterion, the matrices used in this work can be ordered by decreasing Stokes shift: 4-HCCA (10,290-cm^{-1} Stokes shift), caffeic acid (10,007 cm^{-1}), sinapic acid (9274 cm^{-1}), ferulic acid (8738 cm^{-1}), and gentisic acid (7513 cm^{-1}). With the exception of caffeic acid, the Stokes shift data are in nearly perfect anticorrelation with the aerosol MALDI result. There are inconsistencies between the Stokes shift data and solids probe MALDI results as well: Ehring and Sundqvist note that the matrix 3-hydroxy picolinic acid has a Stokes shift of 10,185 cm^{-1} yet typically gives little PSD [32].

There are two mechanisms that can be used to explain the matrix dependence of the prompt fragmentation data: energy transferred to the analyte due to an exothermic proton transfer reaction and collisions in the ablation plume. Energy transfer to the analyte on proton transfer has been suggested as an explanation of matrix dependent fragmentation of vitamin B_{12} by solids probe MALDI [20]. In another study, an exothermic gas phase proton transfer mechanism was used to explain matrix dependent PSD fragmentation of glycoproteins [31]. In the latter work, the plume collision mechanism was rejected because different laser irradiances had little effect on the extent of glycoprotein fragmentation. However, the exothermic proton transfer mechanism does not help to explain the differences between solids probe MALDI and aerosol MALDI fragmentation. Specifically, it fails to explain why the same matrix causes different analyte activation in solids probe MALDI as compared to aerosol MALDI.

The ablation plume collision mechanism is simpler than the proton mechanism in that it is physical rather than chemical and does not presuppose that ionization occurs in the gas phase. Matrix dependent ablation plume density has been used previously to explain the different levels of PSD fragmentation observed with different matrices [4]. It is easy to imagine that the plume density will be different for different matrices due to different absorption coefficients, different melting and sublimation energies, or the different matrix fragments produced by laser desorption. Additionally, sample morphology can affect the amount of material ejected by laser desorption. For example, ganglioside fragmentation was found to vary from spot to spot on a solids probe surface and also from sample to sample [5]. Oligonucleotide ionization efficiency is also highly sensitive to sample morphology and these effects are believed to be related to analyte fragmentation [7, 33].

Different ablation plume densities can lead to different analyte ion internal energies for several reasons. Analyte heating occurs during ablation of ionic and

neutral molecules and in subsequent ion–neutral collisions during acceleration. Neutral molecules produced by MALDI have in some cases been found to have internal energies corresponding to temperatures in excess of 400 K [34]. Conversely, plume collisions may in some cases lead to cooling in a jet expansion of ablated material. For example, rotational cooling in laser desorption has been demonstrated with cryogenic NO films [35]. It has also been shown that the addition of a sugar co-matrix to gentisic acid results in greatly improved mass resolution in Fourier transform mass spectrometry MALDI [36]. It is believed that the sugar co-matrix is pyrolized at a relatively low temperature and the resulting small molecules lead to collisional cooling in the desorption plume. Collisional cooling in laser desorption has been modeled by using a hydrodynamic "cool plume" mechanism [37]. These results suggest a complex process in which different matrices may have different propensities for *both heating and cooling* of an analyte molecule.

The differences in analyte activation for the same matrix between solids probe and aerosol MALDI suggest that the physical plume collision model is more consistent with the aerosol MALDI data than the matrix-specific exothermic proton transfer mechanism. The different fragmentation propensities in solids probe and aerosol MALDI may result from differences in crystallization and the resulting sample morphology. Solids probe MALDI samples are produced by slow evaporation of solvent, whereas aerosol MALDI samples are produced by rapid drying after aerosol formation. It is likely that the crystals formed by rapid solvent evaporation are not the same as those formed by slow solvent evaporation. The different crystal morphologies for aerosol MALDI and solids probe MALDI could lead to different plume densities and hence analyte activation. It is known that some amount of residual solvent is present in the aerosol particles when they are irradiated [23], and this residual solvent may also play a role in plume collisional activation. Because a high acceleration field is present in the aerosol MALDI experiment, it is likely that collisional heating rather than adiabatic expansion cooling is the dominant process. Note that the foregoing argument should not be taken to imply that exothermic proton transfer reactions do not play a role in analyte activation, only that reaction thermodynamics alone seem insufficient to explain the results of the current study.

Conclusions

Aerosol MALDI provides a unique perspective from which to study fundamental laser desorption ionization processes. Aerosol ionization eliminates substrate effects, provides a consistent and constantly renewed sample, and can be used over a wide range of laser irradiances. Notable results of this study are the observation of cobalt removal from the vitamin B_{12} molecule and matrix dependent prompt fragmentation. Cobalt was observed both as free Co^+ as well as in small methanol clusters as $Co^+(CH_3OH)_n$. The metal removal occurs by direct laser desorption without matrix, but is enhanced by the presence of matrix. A small signal corresponding to the demetalated vitamin B_{12}, $[M - Co + H]^+$, is also observed.

Matrix dependent prompt fragmentation of vitamin B_{12} was observed. This fragmentation occurs in the ion source on a time scale of approximately 100 ns and is weakly dependent on laser irradiance. The ratio of peak area of the protonated analyte $[M + H]^+$ and the protonated analyte that has lost the axial CN ligand, $[M - CN + H]^+$, was taken as an indication of the analyte activation during desorption ionization. By this criterion, the matrices 4-nitroaniline and 4-HCCA produce less analyte activation, whereas sinapic, ferulic, caffeic, and gentisic acids produced more analyte activation. Either plume collisions or exothermic proton transfer chemistry can be used to account for matrix dependent analyte activation. The plume collision model is more consistent with the observation from the current study that some matrix molecules give rise to different analyte activation in solids probe MALDI as compared to aerosol MALDI. It is tentatively suggested that this difference is due to the physical differences in the samples, rather than differences in reaction thermodynamics. Previous reports exist in support of both the plume collision and proton transfer mechanisms [4, 20, 31]; further work will be necessary to determine the relative contributions of both processes in MALDI.

Acknowledgments

This research was supported by Emory University and the Emory University Research Committee. The authors wish to thank the American Society for Mass Spectrometry and Finnigan Corporation for an ASMS Research Award and the Society of Analytical Chemists of Pittsburgh for an SACP Starter Grant Award.

References

1. Hillenkamp, F.; Karas, M.; Beavis, R. C.; Chait, B. T. *Anal. Chem.* **1991,** *63,* 1193A–1203A.
2. Senko, M. W.; McLafferty, F. W. *Ann. Rev. Biophys. Biomol. Struct.* **1994,** *23,* 763–785.
3. Spengler, B.; Kirsch, D.; Kaufmann, R. *J. Phys. Chem.* **1992,** *96,* 9678–9684.
4. Kaufmann, R.; Kirsch, D.; Spengler, B. *Int. J. Mass Spectrom. Ion Processes* **1994,** *131,* 355–385.
5. Juhasz, P.; Costello, C. E. *J. Am. Soc. Mass Spectrom.* **1992,** *3,* 785–796.
6. Brown, R. S.; Lennon, J. J. *Anal. Chem.* **1995,** *67,* 3990–3999.
7. Huth-Fehre, T.; Gosine, J. N.; Wu, K. J.; Becker, C. H. *Rapid Commun. Mass Spectrom.* **1992,** *6,* 209–213.
8. Schneider, K.; Chait, B. T. *Org. Mass Spectrom.* **1993,** *28,* 1353–1361.
9. Nordhoff, E.; Karas, M.; Cramer, R.; Hahner, S.; Hillenkamp, F.; Kirpekar, F.; Lezius, A.; Muth, J.; Meier, C.; Engels, J. W. *J. Mass Spectrom.* **1995,** *30,* 99–112.
10. Zhu, L.; Parr, G. R.; Fitzgerald, M. C.; Nelson; C. M.; Smith, L. M. *J. Am. Chem. Soc.* **1995,** *117,* 6048–6056.

11. Nelson, R. W.; Rainbow, M. J.; Lohr, D. E.; Williams, P. *Science* **1989,** *246,* 1585–1587.
12. Romano, L. J.; Levis, R. J. *J. Am. Chem. Soc.* **1991,** *113,* 9665–9667.
13. Tang, K.; Taranenko, N. I.; Allman, S. L.; Chen, C. H.; Cháng, L. Y.; Jacobson, K. B. *Rapid Commun. Mass Spectrom.* **1994,** *8,* 673–677.
14. Tang, K.; Taranenko, N. I.; Allman, S. L.; Cháng, L. Y.; Chen, C. H. *Rapid Commun. Mass Spectrom.* **1994,** *8,* 727–730.
15. Macfarlane, R. D.; Torgerson, D. F. *Science* **1976,** *191,* 920–925.
16. Schulten, H.-R.; Schiebel, H. M. *Naturwissenschaften* **1978,** *65,* 223–230.
17. Barber, M.; Bordoli, R. S.; Sedgewick, R. D.; Tyler, A. N. *Biomed. Mass Spectrom.* **1981,** *8,* 492–495.
18. Ens, W.; Standing, K. G.; Chait, B. T.; Field, F. H. *Anal. Chem.* **1981,** *53,* 1241–1244.
19. Solouki, T.; Russell, D. H. *Appl. Spectrom.* **1993,** *47,* 211–217.
20. Kinsel, G. R.; Preston, L. M.; Russell, D. H. *Biol. Mass Spectrom.* **1994,** *23,* 205–211.
21. Murray, K. K.; Russell, D. H. *Anal. Chem.* **1993,** *65,* 2534–2537.
22. Fei, X.; Wei, G.; Murray, K. K. *Anal. Chem.* **1996,** *68,* 1143–1147.
23. Murray, K. K.; Russell, D. H. *J. Am. Soc. Mass Spectrom.* **1994,** *5,* 1–9.
24. Beeson, M. D.; Murray, K. K.; Russell, D. H. *Anal. Chem.* **1995,** *67,* 1981–1986.
25. Beavis, R. C.; Chait, B. T. *Rapid Commun. Mass Spectrom.* **1989,** *3,* 432–435.
26. Gimon, M. E.; Preston, L. M.; Solouki, T.; White, M. A.; Russell, D. H. *Org. Mass Spectrom.* **1992,** *27,* 827–830.
27. Beavis, R. C.; Chaudhary, T.; Chait, B. T. *Org. Mass Spectrom.* **1992,** *27,* 156–158.
28. Murray, K. K.; Lewis, T. M.; Beeson, M. D.; Russell, D. H. *Anal. Chem.* **1994,** *66,* 1601–1609.
29. Ingendoh, A.; Karas, M.; Hillenkamp, F.; Giessmann, U. *Int. J. Mass Spectrom. Ion Processes* **1994,** *131,* 345–354.
30. Lewis, N. J.; Pfaltz, A.; Eschenmoser, A. *Angew. Chem. Int. Ed. Engl.* **1983,** *22,* 735–736.
31. Karas, M.; Bahr, U.; Strupat, K.; Hillenkamp, F.; Tsarbopoulos, A.; Pramanik, B. N. *Anal. Chem.* **1995,** *67,* 675–679.
32. Ehring, H.; Sundqvist, B. U. R. *J. Mass Spectrom.* **1995,** *30,* 1303–1310.
33. Williams, P. *Int. J. Mass Spectrom. Ion Processes* **1994,** *131,* 335–344.
34. Mowry, C. D.; Johnston, M. V. *J. Phys. Chem.* **1994,** *98,* 1904–1909.
35. Cousins, L. M.; Levis, R. J.; Leone, S. R. *J. Chem. Phys.* **1989,** *91,* 5731–5742.
36. Castoro, J. A.; Wilkins, C. L. *Anal. Chem.* **1993,** *65,* 2621–2627.
37. Vertes, A.; Gijbels, R. In *Laser Ionization Mass Analysis;* Vertes, A.; Gijbels, R.; Adams, F., Eds.; Wiley: New York, 1993; *Chem. Anal.* **1941,** *124,* 127–175.